Two-step Unconventional Protocol for Epitaxial Growth in One Dimension with Hindered Reactions, with Implications For Experiments

Julián A. Sánchez* and Diego Luis González†

Departamento de Física, Universidad del Valle, A.A. 25360, Cali, Colombia

T. L. Einstein‡

Department of Physics and Condensed Matter Theory Center,
University of Maryland, College Park, MD 20742-4111 USA
(Dated: October 19, 2019)

We study the effect of hindered aggregation and/or nucleation on the island formation process in a two-step growth protocol. In the proposed model, the attachment of monomers to islands and/or other monomers is hindered by additional energy barriers which decrease the hopping rate of the monomers to the occupied sites of the lattice. For zero and weak barriers, the attachment is limited by diffusion while for strong barriers it is limited by reaction. We describe the time evolution of the system in terms of the monomer and island densities, N_1 and N. We also calculate the gap length, the capture zone and the island distributions. For all the sets of barriers considered, the results given by the proposed analytical model are compared with those from kinetic Monte Carlo simulations. We found that the behavior of the system depends on the ratio of the nucleation barrier to the aggregation barrier. The two-step growth protocol allows more control and understanding on the island formation mechanism because it intrinsically separates the nucleation and aggregation processes in different times regimes.

I. INTRODUCTION

The study of growth processes has attracted the attention of the scientific community not only because of their academic importance but also for their industrial applications. For instance, epitaxial growth (EG) is used in film growth to fabricate nano and micro-electronic devices. EG involves intriguing out-of-equilibrium phenomena which are not yet fully understood. For instance, the functional forms and the information about the growth process contained in some measurable quantities, such as capture zones, gap lengths and island size distributions, have generated some controversy and discussion [1–7]. For these reasons, it is not surprising to find several theoretical studies devoted to this subject in one dimension (1D) [6–14] and in two dimensions (2D) [1–5, 15–25]. Experimental studies in 1D and 2D can be found in [26–39] and [40–46], respectively. A principal focus of these works is to understand the microscopic mechanisms involved in growth. This is a fundamental requirement to achieve control of the properties of the formed material. Basic models of growth involve three fundamental processes: mass transport (diffusion), formation of stable clusters (nucleation), and growth of stable clusters (aggregation) [5–8, 20, 47]. The basic growth units (atoms or molecules) are usually called monomers and the stable clusters are called islands. Most of the studies about island formation are based on a one-step growth protocol (1SG) where the monomers are deposited at a controlled

———————

* julian.a.sanchez@correounivalle.edu.co
† diego.luis.gonzalez@correounivalle.edu.co
‡ einstein@umd.edu

constant rate F. After deposition, the monomers diffuse over the substrate and eventually begin to interact, forming clusters.

In the standard 1SG protocol, for short times the system evolves basically by nucleation. Thus, in this regime the relevant processes are nucleation, deposition, and diffusion. Consequently, at least three time scales are required to describe the microscopical processes. For long times, the system reaches a quasi steady state where the the density of monomers is much smaller than that of that islands. Thus, the nucleation term in the rate equation for the density of monomers can be neglected in comparison to the aggregation term [6, 8, 18, 48]. Therefore, the time scale associated with aggregation has to be also taken into account. In an effort to make easier the control and understanding of the growth processes, a entirely new deposition protocol has been recently proposed by Tokar and Dreyssé in Ref. [14]. Basically, their protocol consists of two different steps of growth (2SG). In the first step, a small quantity of monomers are deposited simultaneously on the substrate. Experimentally, this can be done by a fast deposition of monomers onto a substrate at low temperature in such way that the hopping rate is negligible. After deposition, the temperature of the substrate is raised, increasing the diffusivity; thus, the monomers diffuse and eventually form islands. Note that, at the end of the first step, the system reaches an equilibrium state characterized by the absence of free monomers. In the second step, additional monomers are deposited sequentially at a constant rate F. Those monomers predominantly aggregate onto the islands formed in the first step. In the second step only the aggregations are relevant because the nucleations are rare events because the typical time between consecutive depositions, $\bar{\tau}_d$, is selected in such way that it is much

larger than the typical aggregation time, $\bar{\tau}_a$. Accordingly, the simultaneous presence of two free monomers on the substrate is unlikely. In the 2SG protocol, nucleation and aggregation occur at different times. In the first step, aggregation is negligible while in the second step nucleation is. The physics involved in the 2SG protocol is intrinsically simpler than that of the 1SG, mainly due to the direct separation of reactions into different steps. In 1SG it is common to delineate two stages, which are traditionally identified as transient and steady-state. However, in the 2SG there are actually two different steps of growth. Additionally, it is important to make clear that the 2SG deposition protocol is a theoretical proposal which offers an alternative to the standard 1SG protocol, seeking to offer more control of the formation of islands. To the best of our knowledge, the 2SG protocol has not yet been implemented experimentally.

In the diffusion-limited aggregation (DL, distinct from DLA in fractal growth) regime, nucleation and aggregation are considered instantaneous because the typical times associated with aggregation and nucleation are negligible compared to the diffusion time of a monomer on the substrate. Most of the literature is devoted to the DL regime [1–25]. However, there are experimental results which suggest the existence of additional nucleation and/or aggregation energy barriers [27–30, 34–41, 49, 50].

For high enough barriers, the typical reaction time can be much longer than the diffusion time; this is the reaction-limited regime (RL) [48, 51–58]. In the RL regime, the monomers require many attempts before attach to a cluster/monomer. Thus, the free monomers density is more spatially uniform in the RL regime than in the DL regime. The description of island formation in the 1SG protocol for the DL and RL regimes leads to a complex set of self-consistent equations which have to be solved numerically because it is not possible to find analytical expressions for the quantities of interest [6, 18, 19, 59].

There are basically two ways to model the attachment/interaction range. In the Shi, Shim, and Amar model (SSA model) [15], in order to react a monomer must hop onto an already occupied site. In contrast, the model proposed by Evans and Bartelt (EB model) [24] includes an implicit short-range interaction. In the EB model a monomer reacts if reaches a site which is the nearest neighbor of an occupied site. Thus, in the SSA model there is no short-range interaction while in the EB there is what amounts to a very strong nearest-neighbor attraction. In this paper our simulations use the SSA model.

Motivated by the work of Tokar and Dreyssé in Ref. [14], and based on previous theoretical and experimental work [48, 57–59, 61, 62], we present a one-dimensional growth model based on the 2SG protocol where nucleation and/or aggregation are hindered by additional energy barriers. For zero and weak barriers, the system is in the DL regime, while for large barriers the system reaches the RL regime. In the limit $\bar{\tau}_d \gg \bar{\tau}_a$, the physics

involved in the second step of the 2SG protocol is much simpler than that in the first step. In this limit, the second step can be understood from the analytical study of a single monomer diffusing between two islands. In contrast, in the first step the nucleation process in which there are several monomers must be addressed. Taking this into account along with the formation of almost all the islands in the first step, we focus this paper on the first step of the 2SG protocol. We emphasize that this work is a theoretical exploration of the capabilities of the 2SG protocol; thus, most of our results can not be applied and/or compared directly to previous studies based on the 1SG protocol.

This paper is organized as follows. In Sec. II the considered model is explained in detail. In Sec. III an analytical study of the model is presented. In Sec. IV the results of extensive kinetic Monte Carlo (kMC) simulations are compared with those from the analytical expressions. Finally, in Sec. V we present some conclusions and an illustrative example of how our model can be applied. In particular, we use an analytical expression for the island size distribution to describe experimental data on the formation of one-dimensional atomic Ag wires on a Pt(997).

II. MODEL DESCRIPTION

In order to describe the first step of growth in the 2SG protocol, we consider a one-dimensional defect-free substrate with length L. At $t = 0$, a small number of mobile monomers are randomly and simultaneously deposited. After deposition, the monomers diffuse with a diffusion constant D_0. Eventually, the monomers meet, forming stable clusters called islands. This process is known as nucleation. Distinctively in 1D, the islands divide the substrate into independent sections called gaps [6–14]. For the sake of simplicity we assume a critical nucleus size $i = 1$; i.e., in our model just two monomers are required to form a stable and static island. An aggregation event occurs when a mobile monomer is captured by an island. This process increases the island size by one unit. Monomers which belong to an island do not diffuse. Given that the initial density of monomers is small, we assume the point-island model, where the islands occupy just a single site on the substrate, and their size is given by the number of monomers which belong to the island. In Refs. [6, 59] it is shown that, for low coverages, the more realistic model of extended-islands gives similar results to those obtained by the point-island model. As mentioned in Sec. I, for short times aggregation is usually negligible and the nucleation is the dominant reaction. However, at the end of the first step there are always some aggregations due to the existence of gaps with a single monomer inside. Therefore, within the first step there are two regimes: the nucleation regime, where almost all the islands are formed, and the second one, where the surviving monomers attach to the existing is-

lands. Eventually, all the mobile monomers disappear because they are captured by the islands. Then, the second growth step begins with the deposition of more monomers at a constant rate F. As usual, the deposition rate satisfies $F \ll D_0$. Thus, the monomers deposited in the second step are more likely to aggregate to the islands formed in the first step than to find and join with another free monomer. In the proposed model the two key reactions, nucleation and aggregation, are hindered by additional energy barriers ϵ_n and ϵ_a, respectively. These barriers act to decrease the hopping rates of monomers to occupied sites of the lattice. Thus, the hopping rates of a monomer to a site occupied by another monomer and by an island are given by $D_n = D_0 \exp(-\epsilon_n/(k_B T))$ and $D_a = D_0 \exp(-\epsilon_a/(k_B T))$, respectively. Usually, the asymmetry between the diffusion rates is quantified through the associated lengths, l_n and l_a, which can be written as $D_0/D_n = l_n + 1$ and $D_0/D_a = l_a + 1$ [48, 55, 57–62]. For large values of ϵ_n and ϵ_a, l_a, $l_n \gg 1$, the nucleation and aggregation are hindered and the system is in the RL regime. In this regime, monomers require many attempts in order to be incorporated into the monomers/islands. In contrast, for zero and weak barriers the system is set in the DL regime and the monomers attach to the monomers/islands once they reach the interaction range.

There are several quantities which can be used to characterize the properties of the growth process. Two are the density of islands with size s, N_s, and the density of monomers, N_1. Both densities give information about the average rates associated with nucleation and aggregation processes. From N_s, it is possible to define the island size distribution $P_s = N_s/N$ with $N = \sum_{s>1} N_s$ the total density of islands. A particularity of the 1D systems is that the islands divide the substrate into independent segments called *gaps*. As a consequence of this geometrical constraint, each monomer inside a given gap must eventually either aggregate to one of the islands at one end of the gap or meet another monomer to nucleates forming a new island inside the gap. The segment between bisections of the gaps at both sides of a given island defines its capture zone. The structure formed by the islands can be partially characterized in terms of the gap length and capture zone distributions, $p_g(\ell)$ and $P_{CZD}(y)$, respectively. These two distributions are related in a non-trivial and unknown way. However, they can be measured experimentally, and therefore, can be used to obtain from experimental results information about the growth processes, such as the key microscopic parameters. We emphasize that the formation of islands in the second step is negligible; thus, the structure formed by the islands only depends on the first step. For this reason we focus on the study of the first step of growth in the 2SG protocol.
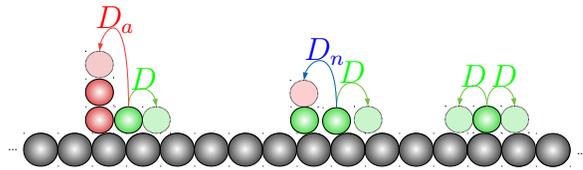

FIG. 1: Schematic representation of the basic processes in the first step of growth. The point-islands are represented by red spheres and occupy just one lattice site. The monomers are represented by green spheres. For leftward arrows, the illustrated processes are, from left to right, aggregation, nucleation, and diffusion to empty sites. The green arrows represent hops to an empty site (diffusion), the blue arrow a hop to a site occupied by a monomer (nucleation) and the red arrow a hop to a site occupied by an island (aggregation).

III. ANALYTICAL MODEL FOR THE FIRST STEP

A. Rate Equations

The time evolution of N_1 and N_s in the first step can be described by standard rate equations (RE) [6, 8, 18, 64, 65]. For N_1 we can write

$$\frac{dN_1}{dt} = -2 k_u N_1^2 - N_1 \sum_{s \geq 2} k_s N_s, \quad (1)$$

where the first term in the right side of Eq. (1) represents nucleation while the second one takes into account the aggregation. The time-dependent factors k_u and k_s are the capture rates for nucleation and aggregation, respectively. In the same way, the evolution of N_s is given by

$$\frac{dN_s}{dt} = N_1(k_{s-1} N_{s-1} - k_s N_s), \quad (2)$$

where $k_{s=1} = k_u$ [59]. The two terms of Eq. (2) represent the aggregation of monomers to islands with size $s-1$ and s, respectively. Let θ_0 be the initial density of monomers. Thus, at $t = 0$, the densities satisfy $N_1 = \theta_0$ and $N_s \approx 0$. The total density of islands is defined by $N = \sum_{s \geq 2} N_s$. Equations (1) and (2) can be written in terms of N as follows:

$$\frac{dN_1}{dt} = -2 k_u N_1^2 - \bar{k} N_1 N, \quad (3)$$

and

$$\frac{dN}{dt} = k_u N_1^2. \quad (4)$$

In Eq. (3) the average aggregation rate, $\bar{k}$, is defined as

$$\bar{k} = \frac{1}{N} \sum_{s \geq 2} k_s N_s. \quad (5)$$

Adding Eqs. (3) and (4), and integrating the result with respect to the time, we arrive at:

$$N_1(t) + 2N(t) = \theta_0 - \int_0^t dt\, \bar{k}\, N_1\, N. \qquad (6)$$

The solution of the RE depends on the relative values of the barriers associated with nucleation and aggregation, which in turn are given by the characteristic lengths l_a and l_n. We considered four different cases: weak and zero barriers ($l_n = l_a = 0$), strong aggregation barrier ($l_a \gg 1$ and $l_n = 0$), strong nucleation barrier ($l_n \gg 1$ and $l_a = 0$), and strong barriers ($l_n, l_a \gg 1$). No matter the value of the barriers, nucleation is the dominant reaction for short times, while aggregation is dominant for long times. Thus, for short times, the REs can be reduced to:

$$\frac{dN_1}{dt} \approx -2\, k_u\, N_1^2 \quad \text{and} \quad \frac{dN}{dt} \approx k_u\, N_1^2, \qquad (7)$$

and Eq. (6) reduces to $2N + N_1 \approx \theta_0$, implying that there are just islands with size $s = 2$. For long times, the nucleation is negligible; thus, aggregation is the relevant process:

$$\frac{dN_1}{dt} \approx -\bar{k}\, N_1\, N \quad \text{and} \quad \frac{dN}{dt} \approx 0. \qquad (8)$$

However, in order to make analytic progress solving the REs, the time dependence of k_u and k_s must be estimated by taking into account the spatial fluctuations of the density of monomers.

B. Nucleation Rate

As mentioned before, for the 2SG protocol, the nucleation regime occurs at short times in the first step of growth. An equivalent way to write Eq. (7) is

$$\frac{dN_1}{dt} \approx -D_0 \frac{N_1}{\xi^2}, \qquad (9)$$

with ξ the capture length of monomers associated with nucleation. On the other hand, the local density of monomers $\eta_1(x,t)$ around a given monomer placed at $x = 0$, evolves according to [10, 15, 17–19]:

$$\frac{\partial \eta_1}{\partial t} = D_0 \frac{\partial^2 \eta_1}{\partial x^2} - D_0 \frac{\eta_1}{\xi^2}, \qquad (10)$$

Subtracting Eq. (9) from Eq. (10) and using the approximation $\partial \eta_1/\partial t \approx dN_1/dt$, we can eliminate the time dependence:

$$\frac{\partial^2 \eta_1}{\partial x^2} - \xi^2 (\eta_1 - N_1) \approx 0, \qquad (11)$$

with boundary conditions $\eta_1(\infty) = N_1$ and $\eta_1(0) = l_n\, \partial \eta_1(x)/\partial x|_{x=0}$ [48, 57–59, 63]. The solution of this differential equation is given by:

$$\eta_1(x) = N_1 \left(1 - \frac{\exp(-x/\xi)}{\frac{l_n}{\xi} + 1}\right). \qquad (12)$$

Now, by comparing the global and local nucleation rates, we can calculate the nucleation rate [6]:

$$2\, k_u\, N_1 = 4\, D_0 \left.\frac{d\eta_1}{dx}\right|_{x=0}, \qquad (13)$$

which gives:

$$k_u = \frac{2\, D_0}{\xi + l_n}. \qquad (14)$$

From Eqs. (7) and (9) the capture length and the nucleation rate are related by

$$\xi^{-2} = \frac{2\, N_1\, k_u}{D_0}. \qquad (15)$$

Using Eqs. (14) and (15) we obtain

$$\xi = \frac{1 + \sqrt{1 + 4\, N_1 l_n}}{8\, N_1}. \qquad (16)$$

Using Eqs. (14) and (16), we find that, for zero and weak barriers $k_u = 8\, D_0\, N_1$, while for strong barriers $k_u = 2\, D_0/l_n$ becomes time independent.

C. Aggregation Rate

For long times, the first step of the 2SG protocol is dominated by the aggregation of monomers which were unable to find another monomer with which to nucleate. Thus, we can write the following equation for the time evolution of monomers at position x inside of a gap of size y, $n_1(x;t)$ [66, 67]:

$$\frac{\partial n_1(x;t)}{\partial t} = D_0 \frac{\partial^2 n_1(x;t)}{\partial x^2}, \qquad (17)$$

with boundary conditions:

$$\begin{aligned}
n_1(0;t) &= l_a \frac{\partial n_1(0;t)}{\partial x}, \\
n_1(y;t) &= -l_a \frac{\partial n_1(y;t)}{\partial x}.
\end{aligned} \qquad (18)$$

The solution of this differential equation depends strongly on the value of l_a. The aggregation rate $\bar{k}$ can be calculated as follows. From the solution of Eq. (17), the average density of monomers can be estimated from

$$\bar{n}_1(y) = \frac{1}{y} \int_0^y dx\, n_1(x;t) \qquad (19)$$

Thus, the total number of monomers on the substrate, $\mathcal{N}_1$, can be calculated from [59, 63]:

$$\mathcal{N}_1 = \sum_y \bar{n}_1 p_g(y)\mathcal{N}, \qquad (20)$$

and the associated average density, $N_1 = \mathcal{N}_1/L$, is given by

$$N_1 = N\langle \bar{n}_1\, y \rangle, \tag{21}$$

where the $\langle \cdots \rangle$ denotes an average over the distribution of gaps. Equation (21) implicitly contains information about the aggregation time τ_a. However, we note that calculation of the mean value in Eq. (21) requires knowledge of the gap-length distribution, $p_g(y)$.

D. Gap size distribution

Since few monomers are deposited randomly onto the substrate in the first step, the nucleations can reasonably be considered to be uncorrelated events. Under this assumption, $p_g(\ell)$ can be calculated from the convolution of two gap-length distributions between a pair of adjacent monomers, $q(\ell)$. In order to illustrate this idea, we consider two neighboring monomers of a given island, as shown in Fig. 2. We assume that both ℓ_1 and ℓ_2 follow the distribution $q(\ell)$. Inspired by the Gruber-Mullins approximation [68], we allow just the monomer in the middle to be mobile. Thus, nucleation occurs when the mobile monomer reaches the static monomer.

Naturally, nucleations can occur in other positions; therefore, our approximation underestimates the variance of $p_g(\ell)$. The probability that a nucleation event creates a gap of length ℓ is given by:

$$p_g(\ell) = \int d\ell_1\, d\ell_2\, q(\ell_1)\, q(\ell_2)\, \delta(\ell - (\ell_1 + \ell_2)). \tag{22}$$

Under the assumption that the positions of the monomers are uncorrelated, the length distribution between consecutive monomers is given by $q(\ell) = a\,\theta_0 \exp(-a\,\theta_0\,\ell)$ with $0 < a < 1$ a time dependent parameter which is related with the fraction of nucleated monomers. In this way, the average distance between two consecutive monomers is $1/(a\,\theta_0)$ with $a\,\theta_0$ the fraction of non-nucleated monomers. Consequently, the gap length distribution between adjacent islands can be written as:

$$p_g(\ell) = a\,\theta_0^2\,\ell \exp(-a\,\theta_0\,\ell). \tag{23}$$

For $t = 0$, there are no islands implying $a = 2\,N_1/\theta_0$ while for long times there are no monomers and $a = 2\,N/\theta_0$.

The gap length distribution gives information about nucleation around a given island. In general, $p_g(\ell)$ can be written in the form:

$$p_g(\ell) = c(\ell) \exp\left(-\int_0^\ell c(y)dy\right), \tag{24}$$

with $c(x)$ the density of islands at a distance x from a given island at position $x = 0$. Naturally, $c(x)$ is related to the probability of nucleation; for example, in the mean-field (MF) approximation the probability of nucleation is written as the square of the density of monomers, i.e., $c(x) \sim n_1(x,t)^2$.
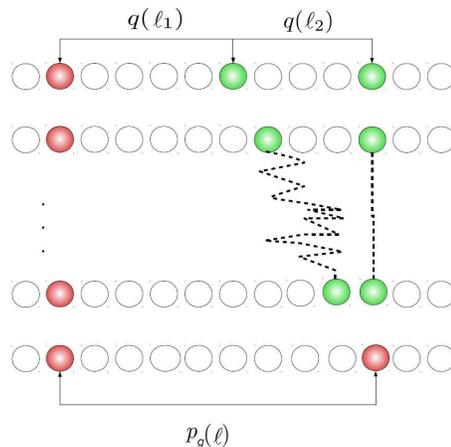

FIG. 2: Scheme of the nucleation process in the case where the positions of the monomers are uncorrelated. As before, the islands and monomers are represented by red and green spheres, respectively.

E. Island size distribution with constant rates

The island size distribution $P_s = N_s/N$ can be determined explicitly from the REs in the case of time-independent rates as follows. First, we suppose that $k_s = \bar{k}$ for all s, which is valid for point islands. Second, we assume that the aggregations begin when all the islands are formed only by two monomers, thus $P_s = \delta_{s,2}$. Finally, we assume that for long times the nucleations are rare events, so that the total number of islands can be considered constant. Under these approximations and using the change of variable $\tau = \int_{t_c}^t dt\,\bar{k}\,N_1$, the REs are reduced to:

$$\frac{dN_s}{d\tau} = N_{s-1} - N_s, \tag{25}$$

and

$$\frac{dN_2}{d\tau} = -N_2, \tag{26}$$

with t_c the crossover time between nucleation and aggregation, and $N_2(\tau = 0) = N\delta_{s,2}$. Now, after a Laplace transform, we find:

$$\tilde{N}_s = \frac{\tilde{N}_2}{(\bar{\tau}+1)^{s-2}}, \tag{27}$$

and

$$\tilde{N}_2 = \frac{N}{(\bar{\tau}+1)}. \tag{28}$$

After taking the inverse Laplace transform and the large-time limit, we can write N_s as:

$$N_s(\tau) = \frac{N}{(s-2)!}\tau^{s-2}\exp(-\tau), \tag{29}$$

Finally, taking $\bar{s} = \sum_{s=2}^{\infty} s \, P_s$, we see that $\bar{s} = \tau + 2$. Equation (29) gives a parametric expression for the island size distribution, where the parameter $\bar{s}$ is the average size of islands.

IV. RESULTS AND DISCUSSION FOR THE FIRST STEP

A. Case I: Weak and zero barriers ($l_n = l_a = 0$)

As shown by Eq. (14), for short times and zero barriers, $k_u \sim N_1$. Consequently, the solution of the REs in this regime is given by:

$$N_1 \approx \left(\frac{1}{32 \, D_0 \, t + \theta_0^{-2}} \right)^{1/2} \quad \text{and} \quad N \approx \frac{\theta_0}{2} - \frac{1}{2} \left(\frac{1}{4 \, D_0 \, t + \theta_0^{-2}} \right)^{1/2} . \quad (30)$$

On the other hand, the explicit solution of Eqs. (17) and (18) satisfies [66, 67]:

$$n_1(x;t) = \sum_{m=0}^{\infty} \frac{4 \, \theta'}{\pi(2m+1)} e^{-\frac{(2m+1)^2 \pi^2 D_0 t}{y^2}} \sin\left[\frac{(2m+1)\pi x}{y}\right], \quad (31)$$

where $y^{-1} \int dx \, n_1(x;0) = \theta'$ is the average density of monomers at the beginning of aggregation regime ($\theta' = N_1(t_c)$).

For long times it is possible to approximate Eq. (31) as:

$$n_1(x;t) \approx \frac{4\theta'}{\pi} \exp\left(-\frac{\pi^2 D_0 t}{y^2}\right) \sin\left[\frac{\pi x}{y}\right]. \quad (32)$$

The average density $\bar{n}_1$ of monomers inside a gap with length y, can be written as:

$$\bar{n}_1 = \frac{1}{y} \int_0^y dx \, n_1(x;t) = \frac{8 \, \theta'}{\pi^2} \exp\left(-\frac{\pi^2 D_0 t}{y^2}\right). \quad (33)$$

From Eq. (33) we conclude that the typical aggregation time for a gap with length y is given by $\tau_a = y^2/(\pi^2 D_0^2)$; which agrees with previous results [48, 58, 61–63]. The mean value in Eq. (21) can be calculated by using the approximate expression for $p_g(\ell)$ given by Eq. (23) and evaluating the resulting integral by means of the saddle-point approximation [66, 67]:

$$N_1 \approx N \int_0^{\infty} dy \, \bar{n}_1 \, y \, p_g(y),$$

$$\sim \int_0^{\infty} dy \, y^2 \, \exp\left(-t \left[\frac{Ny}{t} + \frac{\pi^2 D_0}{y^2}\right]\right)$$

$$\sim t^{-1/6} \exp\left(-\frac{3}{2} \left(2\pi^2 N^2 D_0 t\right)^{1/3}\right). \quad (34)$$

The argument of the exponential function gives the average aggregation time in the entire system, $\bar{\tau}_a = 1/(2 \, \pi^2 N^2 D_0)$, which agrees with an earlier study [47]. Taking into account that the average gap length is given

by $\bar{y} = 1/N$, we can write $\bar{\tau}_a = \bar{y}^2/(2 \, \pi^2 \, D_0)$. It is important to note that the local aggregation time, τ_a, is proportional to the square of the gap length, while the global aggregation time $\bar{\tau}_a$ goes like the square of the *average* gap length. Thus, the average aggregation rate can be calculated by inserting Eq. (8) into Eq. (34):

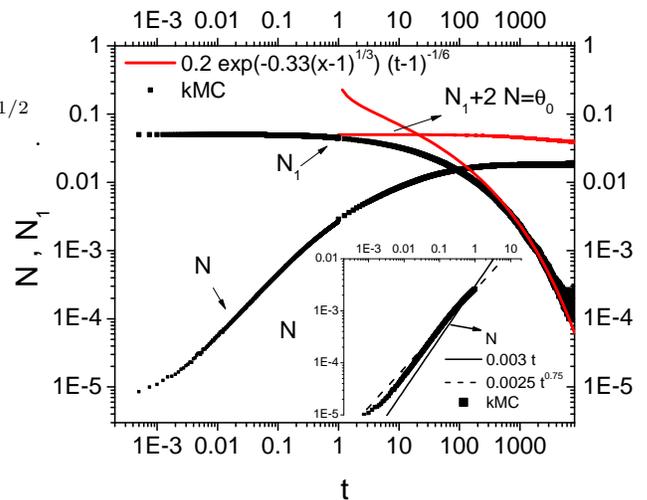$$\bar{k} = \left(\frac{2 \, \pi}{t}\right)^{2/3} \left(\frac{D_0}{N}\right)^{1/3} \quad (35)$$

FIG. 3: Time evolution of the densities N_1 and N for zero and weak barriers ($l_a = l_n = 0$). Dots correspond to kMC results while continuous lines to analytical expressions. The inset shows the behavior of N for short times.

The comparison between the results obtained analytically with those from the kinetic Monte Carlo (kMC) simulations are shown in Fig. 3. The inset shows the behavior for short times, the analytical model suggest $N \sim t$ while the kMC results give $N \sim t^{\delta}$, with the exponent δ between $3/4$ and 1. The predicted slope for short times given by Eq. (30) is about to 2×10^{-3}, which is close to the numerical value suggested by the kMC results. The discrepancies are due to the small but non zero probability to deposit at random two or more consecutive monomers at $t = 0$. The probability of having n consecutive monomers after a random deposition, P_n, satisfies $\theta_0/ \sum_{i=1}^{\infty} m_i = \sum_{i=1}^{\infty} i \, P_i$ where m_i is the number of domains with size i. On the other hand, the probability to deposit n monomers in an equal number of consecutive sites is θ_0^n. Thus, neglecting the formation of monomer domains with length larger than two units, we find that since $\theta_0 \ll 1$, $m_2 \approx \theta_0^3$. Finally, at very short times, about the half of the domains formed by two consecutive monomers will give rise to islands of size two. In our case $\theta_0 = 0.05$, which leads to $m_2 \approx 1.25 \times 10^{-4}$ and $N(0) \sim 10^{-5}$, as shown in Fig. 3. On the other hand, for long times, the fit is excellent, validating the analytical considerations used to write Eq. (34). In writing Eq. (34)

the time origin is taken at $t = t_c$, when the islands are completely formed. Consequently, it is necessary to use a time translation in order to compare Eq. (34) with kMC results. In the main panel the function $N_1 + 2N$ is also included, showing that the aggregation plays an important role for times greater than 10 while for short times the dominant reaction is nucleation, and $N_1 + 2N \approx \theta_0$.

Figure 4 shows the results obtained for the gap length distribution using the scaled distance $\ell \to \ell/\bar{\ell}$. The fit given by Eq. (23) is very good, validating the nucleation mechanism for the formation of gaps illustrated in the Fig. 2. From Eq. (24) the results clearly suggest that the density of monomers becomes constant far from the islands but decreases quickly near them, forming a depletion region. In fact, to recover Eq. (23) from Eq. (24) the argument of the exponential in Eq. (24) must be written as:

$$\int_0^x c(y)\, dy \sim \int_0^x P_n\, dy = P_n\, x, \qquad (36)$$

with $P_n(x) \approx P_n$, where P_n is the uniform nucleation probability at a distance x from a given island. For $x \gg 1$ the nucleation probability must be uniform in such a way that the gap size distribution decays exponentially, as in Eq. 23). On the other hand, for $x \ll 1$ we have that $c(x) \sim x$, so that the density of monomers and therefore the nucleation probability go to zero in the neighborhood of islands. The Eq. (23) shows that the density of islands close to a given island grows linearly with x, implying $P_n \sim x$. However, Eq. (32) predicts a linear behavior for the monomer density close to an island, leading to $P_n \sim x^2$. Thus, the MF approximation for the description of nucleation must not be valid for small values of x. Figure 4 (b) confirms the linear behavior of the left tail of the distribution and the exponential behavior of the right tail. The kMC results support the assumption of statistical independence between consecutive gaps. Thus, the formation events of consecutive islands are uncorrelated because most of the nucleations occur when the system is still well mixed and the density of monomers can be considered homogeneous. In this way, the capture zone distribution, $P_{CZD}(y)$, can be determined from the convolution product:

$$P_{CZD}(y) \approx \int d\ell_1\, d\ell_2\, p_g(\ell_1) p_g(\ell_2) \delta\left(y - \frac{(\ell_1 + \ell_2)}{2}\right), \qquad (37)$$

which gives explicitly

$$P_{CZD}(y) \approx \frac{8}{3} a^4 \theta_0^4 y^3\, \exp(-2\, a\, \theta_0\, y). \qquad (38)$$

The numerical results agree with the formula in Eq. (38); see Fig. 4(c). Finally, the behavior of the island size distribution is shown in the Fig. 5. Again, the results obtained from the kMC simulations and the ones given by Eq. (29) agree with each other. Consequently, we conclude that P_s can be determined assuming that k_u and $\bar{k}$ are time independent. We note that the work of Tokar and Dreyssé neglects aggregation in the first step of growth. However, Fig. (5) shows that some aggregation events occur, due to the fact that there are islands with size larger than $s = 2$. This is also suggested by Fig. 3 because $N + 2N_1$ is no longer a constant at long times.

B. Case II: Strong aggregation barrier ($l_a \gg 1$ and $l_n = 0$)

By definition, the aggregation barrier does not affect nucleation. Therefore, the behavior of the system for the short times is the same of that found in Case I given by Eq. (30). Nevertheless, for long times, the aggregation barrier plays an important role by increasing the typical time associated with aggregation. From Eq. (17), the density $n_1(x,t)$ can be calculated following the same procedure used in Case I. In this way, we found

$$n_1(x,t) = B_1 e^{-\frac{2D_0 t}{l_a y}}\left(\sin\sqrt{\frac{2}{l_a y}}x + l_a\sqrt{\frac{2}{l_a y}}\cos\sqrt{\frac{2}{l_a y}}x\right), \qquad (39)$$

with B_1 a parameter dependent on the initial condition. The average density of monomers inside a gap takes the form:

$$\bar{n}_1 \approx \frac{B_1}{y}(2 l_a y)^{1/2} \exp\left(-\frac{2D_0 t}{y\, l_a}\right). \qquad (40)$$

Again, the argument of the exponential function gives the typical aggregation time, $\tau_a = l_a\, y/2\, D_0$, which is much longer than the one found in Case I. For zero and weak barriers, the aggregation time is equal to the typical time that a monomer needs to reach one of the islands at the gap edges.

Using the Eq. (21) in conjunction with $p_g(\ell)$, we can calculate the average density of monomers. Given that the mechanism of island formation is not modified by the existence of the aggregation barrier, it is reasonable to expect that the gap length and capture zone distribution remain close to the ones found in Case I. This can be seen in Fig. 4, which shows that, in the case of a strong aggregation barrier, the kMC results for $p_g(\ell)$ and $P_{CZD}(y)$ are well fitted by the Eqs. (23) and (38), respectively. In fact, the fit is even better than the one found in Case I. As in Case I, the spatial fluctuations are only relevant in the neighborhood of the islands/monomers; they can be neglected far away from the islands. The behavior of the average density of monomers for long times is given by

$$N_1 \approx N \int_0^\infty dy\, \bar{n}_1\, y\, p_g(y), \qquad (41)$$

$$\sim \int_0^\infty dy\, y^{3/2} \exp\left(-t\left[\frac{Ny}{t} + \frac{2D_0}{yl_a}\right]\right), \qquad (42)$$

$$\sim t^{-3/8} \exp\left(-\left[\frac{N D_0 t}{l_a}\right]^{1/2}\right) \sim t^{-3/8}, \qquad (43)$$
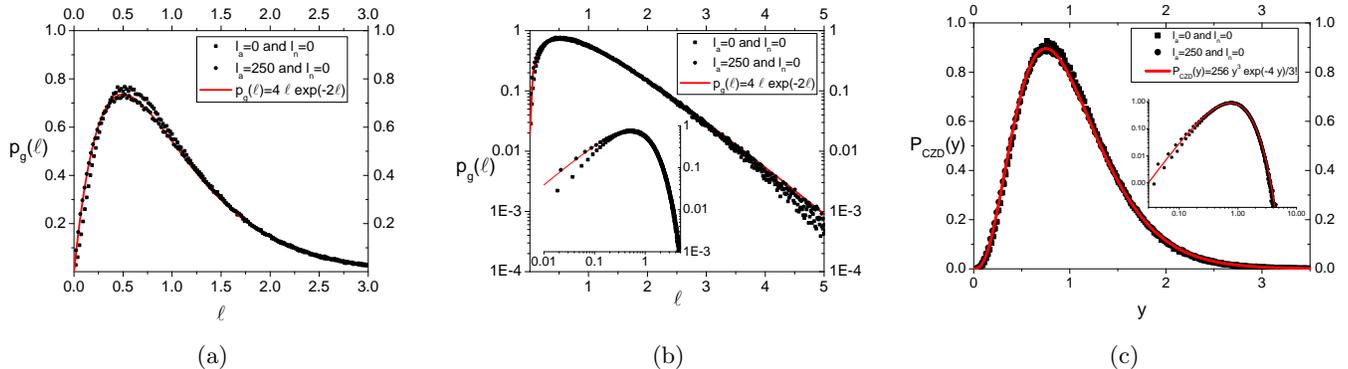
FIG. 4: Gap length distribution and capture zone distribution for cases I and II. As before dots corresponds to kMC results and lines to the analytical approximations. (a) $p_g(\ell)$ for $l_a = l_n = 0$ (squares) and $l_a = 250$ with $l_n = 0$(circles), (b) the same distributions in logarithmic scale to highlight the behavior for large and small values of s. (c) $P_{CZD}(y)$ for the same sets of barriers. The continuous lines in (a) and (b) correspond to Eq. (23) while in (c) to Eq. (38).
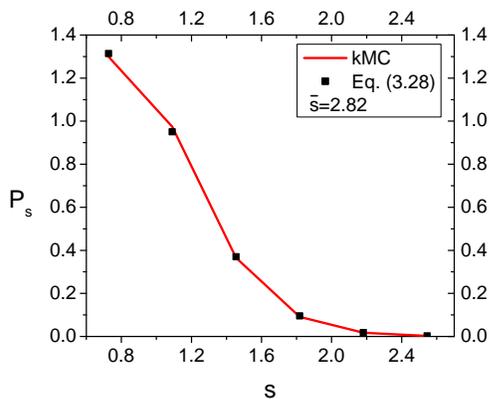

FIG. 5: Comparison between the kMC results for the island size distribution and Eq. (29) for Case I ($l_a = l_n = 0$). Dots represents the results of kMC simulations, while the line represents Eq. (29).

where the condition $N D_0 t / l_a \ll 1$ has been used. After the same process used in Case I, the average aggregation rate takes the form:

$$\bar{k} = \frac{3}{8 t N}. \tag{44}$$

Due to the action of the barrier, aggregation becomes an infrequent event, implying that the approximation $N + 2N_1 \approx \theta_0$ works even better than in Case I. It is also worth noting that N_1 now decays algebraically: $N_1 \sim t^{-3/8}$, see Fig. 6 (a). Additionally, Fig. 6 (b) shows that the existence of the barrier decreases the mean size of the islands because, typically, only islands with very few monomers form. In fact, practically all islands have sizes $s = 2$ and 3. The case of strong aggregation barrier is closer to the ideal model proposed by Tokar and Dreyssé, where the aggregation in the first step of growth is neglected. The results given by Eq. (29) fit well the island size distribution found in kMC simulations.

C. Case III: Strong nucleation barrier ($l_a = 0$ and $l_n \gg 1$)

The nucleation barrier does not affect the behavior of the densities at long times. Nevertheless, the formation process of islands is strongly affected by the barrier. In the limit of strong nucleation barriers, the monomers require many encounters before having a nucleation. The existence of ϵ_n increases the repulsion force between monomers, inducing correlations between their positions. Thus, the simple model of two monomers used in Cases I and II, represented in Fig. 2, is not viable.

As we showed in Sec. III, in the limit of strong nucleation barriers Eq. (14) reduces to $k_u \approx 2 D_0/l_n$. In this way, for short times the global densities take the form:

$$N_1 \approx \theta_0 \left(1 - k_u \theta_0 t\right) \quad \text{and} \quad N \approx k_u \theta_0^2 t. \tag{45}$$

Taking into account that the nucleation barrier does not affect aggregation, we expect that for long times the densities satisfy Eq. (34), as shown in Fig. 7 (a).

Given the effect of the nucleation barrier, we expect that in the aggregation regime most of the islands have size $s > 2$. Then, we propose that $p_g(\ell)$ can be written as the convolution of three $q(l)$ distributions instead of two as in cases I and II. Due to the strong nucleation barrier, it is reasonable to expect that nucleations occur in configurations where there are three consecutive monomers in the neighborhood of a preexisting island. As in cases I and II, we consider just the monomer in the middle as mobile. Due the repulsion of the island, the movement of the mobile monomer is biased in favor of the direction away from the island. Therefore, a new gap is formed when the mobile monomer reaches the monomer furthest from the island. Hence, we propose the following semi-empirical expression based in the convolution of three
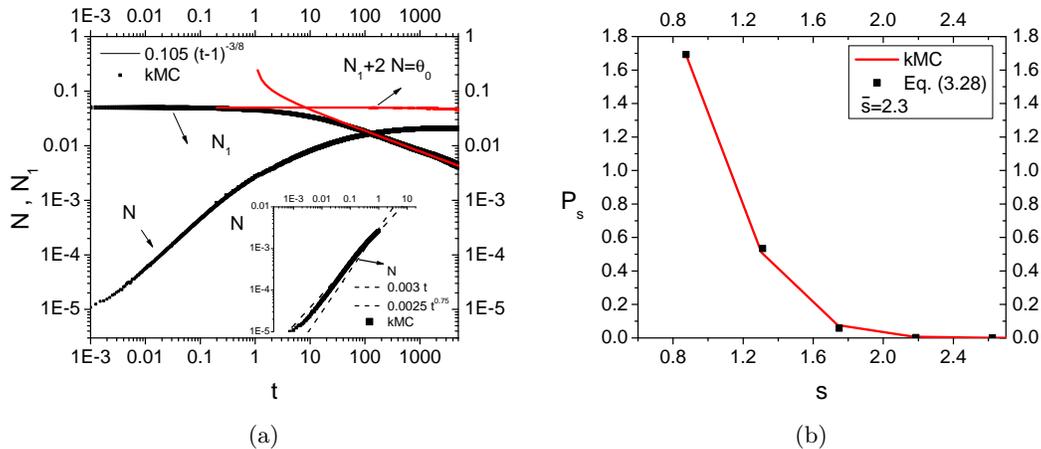
FIG. 6: Results for Case II ($l_a = 250$, $l_n = 0$). (a) Time evolution of the densities N_1 and N. The inset shows the behavior of N for short times. (b) Island size distribution. In both figures, dots corresponds to the results obtained from kMC simulations while continuous lines to analytical expressions.
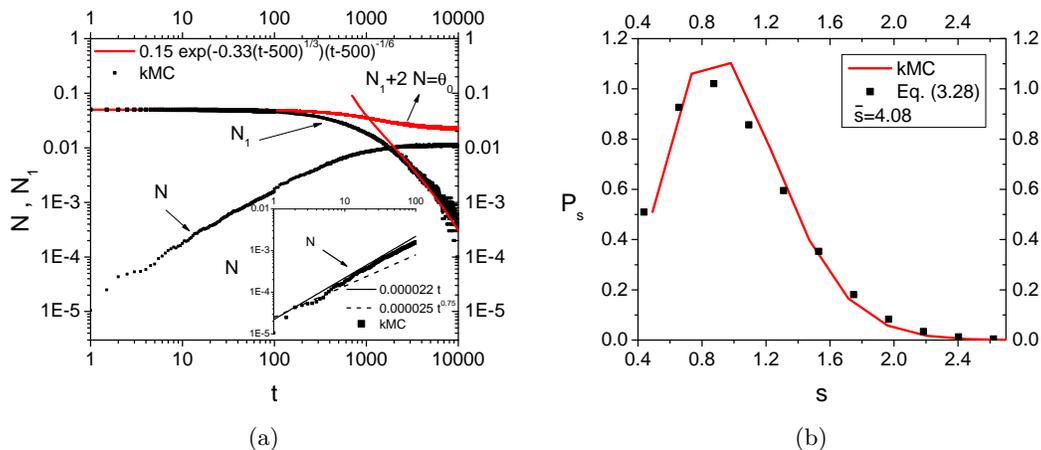

FIG. 7: Results for Case III ($l_a = 0$, $l_n = 250$). (a) Time evolution of the densities N_1 and N. The inset shows the behavior of N for short times. (b) Island size distribution. In both figures, dots correspond to the results obtained from kMC simulations while continuous lines to analytical expressions.

$q(\ell)$ distributions:

$$p_g(\ell) \approx \int \left[\prod_{i=1}^{3} d\ell_i\, q(\ell_i) \right] \delta\left(\ell - (\ell_1 + \ell_2 + \ell_3) \right)$$
$$\approx (1/2) a^3 \theta_0^3 \ell^2 \exp(-a\,\theta_0\,\ell), \qquad (46)$$

rather than the one used in the two previous cases Eq. (23), which is obtained from the convolution of just two $q(\ell)$ distributions. Comparing Eq. (24) with Eq. (46) we conclude that the density of monomers is approximately constant far away from the islands, with important fluctuations in the neighborhood of them; see Fig. 8 (a). The results suggest that, for small x, the island density grows as $c(x) \sim x^2$. In this case, the nucleation rate is $k_u \approx 2\,D_0/l_n \approx 0.008$; consequently, the slope of $N(t)$

is approximately 0.00002. This value is very close to the numerical value found by kMC simulations, see Fig. 7 (a). As expected, given the presence of the nucleation barrier, island formation occurs for later times than in the two previous cases. Additionally, the island size distribution is well described by Eq. (29), with small differences for islands of size $s = 3$.

The effect of the correlations between nucleation events implies a weak time dependence of k_u and $\bar{k}$. Given that the typical time for nucleation is longer than the aggregation one, the aggregations are favored over the nucleations, making possible the formation of islands having several monomers. In that case, the average island size is larger than the ones found in Cases I and II. We emphasize that in this case the gap length distribution is

affected significantly, implying an important change in the nucleation mechanism. In this case, the positions of monomers are correlated, and the fluctuations of the monomer density near the islands are stronger than in Cases I and II. On the other hand, for large gaps, the distribution decays exponentially as before, meaning that the monomer density stays uniform far away from the islands, i.e., for $x \gg \xi$, with ξ the capture length [72]. The capture zone distribution can be calculated satisfactorily as before, i.e., from the convolution of two gap size distributions (Eq.(46)). This means that in spite of correlations between the positions of monomers, the consecutive gaps can be considered statistical independent. This result is consistent with our model for gap formation, where it is only necessary to consider statistically independent spacings between few monomers (two for $l_n = 0$ and three for $l_n \gg 1$) around a given island, regardless of any other islands or monomers of the system.

D. Case IV: Strong barriers ($l_a \gg 1$ and $l_n \gg 1$)

Finally, the case where both nucleation and aggregation barriers are strong is considered. Figures 9 (a) and 9 (b) show the results for the gap length distribution. We note that the distribution decays exponentially for large values of ℓ, in agreement with Eq. (23). In this case, the spatial fluctuations in the neighborhood of islands and monomers are quite important, which is reflected in the slope of $p_g(\ell)$ for small values of ℓ.

The temporal evolution of densities is shown in Fig. 10 (a). For short times, the system behaves very similarly to the case $l_a = 0$ and $l_n = 250$, and nucleation is the dominant process. For late times, the densities have the same behavior as those found in the Case II. The nucleation barrier delays the formation of islands. For late times N_1 only changes by aggregation.

Figure 10 (b) shows the behavior of the densities as a function of time. The scale behavior is found by using the transformation $t \to \tilde{k}\, t$ with $\tilde{k} = k_u = \bar{k}$. This transformation causes the curves for parameters to collapse onto a single curve, as predicted by the RE.

We note that Figs. 3, 6a, 7a, and 10 show that the time at which $N \approx N_1$ satisfies the relation $N(\approx N_1) \approx \theta_0/3$, regardless of the values of the barriers and in agreement with the predictions of Eq. (6). Figure 10c shows the behavior of P_s for four different sets of barriers. The distribution is basically the same for all the sets of barriers. We conclude that the island size distribution seems to be less sensitive to the barrier values than the gap length and capture zone distributions. This is exemplified by comparing $p_g(\ell)$ for the cases $l_a = l_n = 0$ and $l_a = l_n = 250$; see Figs. 4a and 9a. Note that $p_g(\ell)$ is similar for both set of barriers for large values of s, with considerable differences for small values. Many experimental and theoretical works have focused on calculating just the island size distribution or the capture zone distribution. However, our results show that the two distributions give complementary and not necessarily equivalent information about the microscopic processes of the system. Therefore, both distributions should be taken into account to obtain a more complete description of growth.

V. CONCLUSIONS

A brief summary of the key results is shown in Table I. In 2SG, most of the islands are formed in the first step of growth while in the second step the islands just increase their size by aggregation. The 2SG protocol suggested by Tokar and Dreyssé intrinsically separates nucleations from aggregations, allowing us more control and understanding of the growth process. This advantage is more pronounced in the case of large aggregation barriers. In contrast, in 1SG, nucleation and aggregation often occur simultaneously, requiring us to consider many time scales to describe the evolution of the system. Consequently, it is easier to treat 2SG analytically than 1SG.

It is well known in the literature that generally in the systems in the RL regime, the spatial fluctuations can be neglected; consequently, the reaction rates can be taken as constants in the respective REs. However, we found that, for the case in which two monomers form a stable island, the spatial fluctuations in the density of monomers are relevant in the spatial region close to the monomers, even in the case of a strong nucleation barrier. This is not an unexpected result because the nucleation reaction has an upper critical dimension $d_c = 2/i$, while the aggregation reaction has $d_c = \infty$. The effect of the spatial fluctuations in the monomers density is always present in the slope of $p_g(\ell)$ and $P_{CZD}(y)$ for small values of ℓ and y, respectively.

Our results suggest that, in the 2SG protocol, $P_{CZD}(y)$ decays exponentially regardless of the values of the barriers. On the other hand, some of us have argued that the generalized Wigner surmise should account for the CZD [70]. The behavior that we found in this work is quite different from the Gaussian tail of the generalized Wigner surmise [1, 2]. Extensive simulations in one dimension by Shi et al. [15] for the 1SG model and zero barriers found good agreement with the Wigner surmise for the exponent $\beta = 4$ (so no generalization needed):

$$P_{CZD}(y) = (64/9\pi)^3\, y^4 \exp(-(64/9\pi)\, y^2), \qquad (47)$$

with different asymptotic behavior for both small and large y. Additionally, the right tail of the CZD has been studied numerically for the DL regime in the 1SG protocol suggesting $P_{CZD}(y) \sim \exp(-\text{const}\, y^3)$ [7, 9]. From Eq. (24) it is clear that the growth protocol modifies the probability of nucleation around a given island, changing the behavior of $p_g(\ell)$ and $P_{CZD}(y)$. We conclude that the behavior of the CZD is not universal and strongly
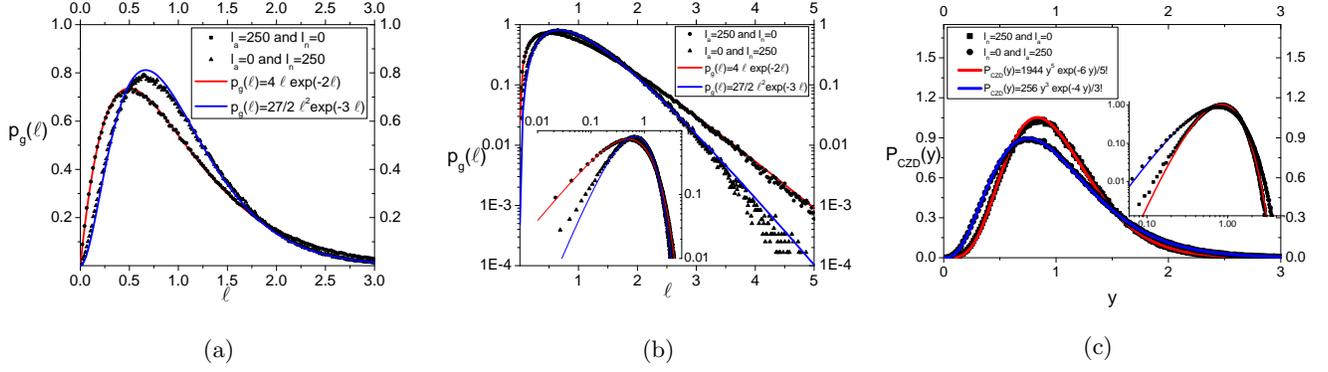
FIG. 8: Gap length distribution and capture zone distribution for Cases II and III. As before dots correspond to kMC results and lines to the analytical approximations. (a) $p_g(\ell)$ for $l_a = 0$, $l_n = 250$ (triangles) and $l_a = 250$ with $l_n = 0$(circles), (b) the same distributions on a logarithmic scale to highlight the behavior for large and small values of ℓ. (c) $P_{CZD}(y)$ for the same sets of parameters.
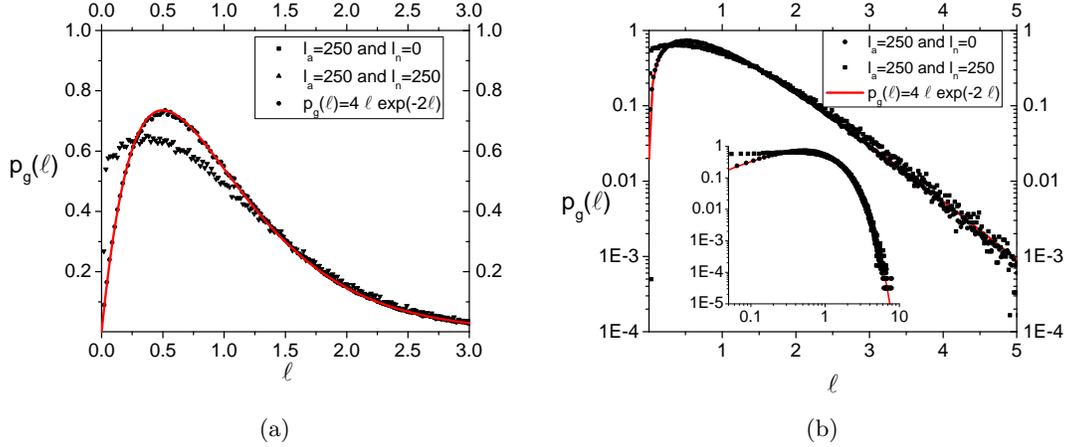

FIG. 9: Gap length distribution for Case IV ($l_a = l_n = 250$). For ease of comparison, Case II ($l_n = 0$, $l_a = 250$) has been included. As before, the sets of points correspond to the kMC results.
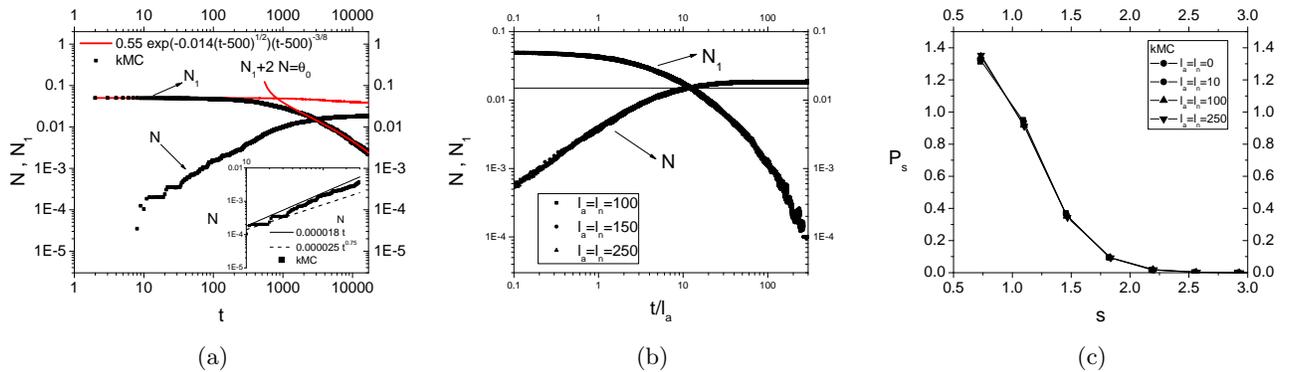

FIG. 10: (a) Time evolution of the densities N_1 and N for Case IV ($l_n = l_a = 250$). (b) Scale behavior of N_1 and N for different sets of barriers which satisfy $l_n = l_a$. (c) Island size distribution for all cases for the same sets of barriers used in panel (b). As before, dots correspond to kMC results and lines to analytical expressions.

depends on the growth mechanism. In the 2SG proto-   col most of the islands are formed when the system is

TABLE I: Key Results

	$l_a = 0$ and $l_n = 0$	$l_a \gg 1$ and $l_n = 0$	$l_a = 0$ and $l_n \gg 1$	$l_a \gg 1$ and $l_n \gg 1$
$p_g(\ell) \sim \ell^{\vartheta}$ with $\ell \ll 1$	$\vartheta = 1$	$\vartheta = 1$	$\vartheta = 1$	$\vartheta \to \infty$
$p_g(\ell) \sim \exp(-\text{const}\,\ell)$ with $\ell \gg 1$	const $= 2$	const $= 2$	const $= 3$	const $= 2$
Eqs. (29) and (37)	Valid	Valid	Valid	Valid
$N_1 \sim t^{-\xi} \exp\left(-\text{const}\,(t/\bar{\tau}_a)^{\zeta}\right)$	$\xi = \frac{1}{6}$ and $\zeta = \frac{1}{3}$	$\xi = \frac{3}{8}$ and $\zeta = 0$	$\xi = \frac{1}{6}$ and $\zeta = \frac{1}{3}$	$\xi = \frac{3}{8}$ and $\zeta = \frac{1}{2}$
$\bar{\tau}_a^{-1}$	$2\pi^2 N^2 D_0$	$N D_0/l_a$	$2\pi^2 N^2 D_0$	$N D_0/l_a$

still well mixed leading to a exponential tail in $p_g(\ell)$ and $P_{CZD}(y)$. In contrast, for the 1SG the numerical evidence suggests that the probability of nucleation around an island cannot be taken as a constant, even at large distances from the island.

The distributions calculated in this work, P_s, $p_g(\ell)$ and $P_{CZD}(y)$, can be determined experimentally. Therefore, these distributions can be used to describe the microscopic processes involved in EG.

Our results suggest that different sets of barriers could lead to the same island size distribution. In order to differentiate those cases, it is necessary to calculate $p_g(\ell)$ and/or $P_{CZD}(y)$, the latter seeming more sensitive to the energy barriers. In all cases, P_s is well described by Eq. (29), which assumes constant kernels and neglects the time dependence due the spatial fluctuations. However, both $p_g(\ell)$ and $P_{CZD}(y)$ can only be well described if the spatial fluctuations of the monomer density are taken into account. In all cases $p_g(\ell)$ decays exponentially implying that P_n can be taken as a constant for points far away from the islands. In contrast, for small distances the monomer density and P_n strongly depend on the distance from the island. It is clear that P_s, $p_g(\ell)$ and $P_{CZD}(y)$ give complementary but not necessarily equivalent information about the microscopic growth processes. Thus, for the analysis of experimental results, those distributions must be considered jointly and not separately, as was done in several previous works.
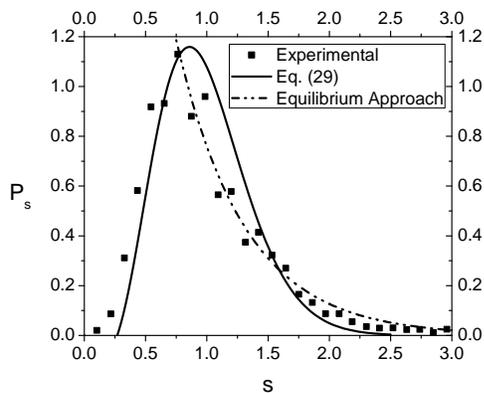

FIG. 11: Comparison between the experimental data and the equilibrium model reported in Ref. [42] with the island size distribution given by Eq. (29).

The spatial fluctuations in the monomer and island densities are more important in one dimension than in higher dimensions. When the spatial dimension is higher than the critical dimension, the monomers tend to remain well mixed. For nucleation, $d_c = 2$ for $i = 1$; thus, neglecting logarithmic corrections, the spatial fluctuations are less important for two dimensional systems than they are for one-dimensional ones. Therefore, the mean-field description of the 1SG presented here should work even better in two-dimensional systems. Thus, we can expect that the advantages offered by the 2SG protocol and discussed in this paper should also be present in the most relevant case of growth on two-dimensional substrates. Finally, we believe that the experimental implementation of 2SG could offer a new approach to the experimental groups which use EG, simplifying the understanding and analysis of the growth processes.

As a closing illustrative example, we consider the rather extensive experimental data in Gambardella et al. [42] on the formation of one-dimensional atomic Ag wires on a Pt(997) surface, with an array of steps with very few kinks and nearly uniform terrace widths. Because of the increased binding energy at step sites, monomers deposited on vicinal surfaces can self-assemble—for suitable temperature—into chain-like structures along the step edges. In this case, there is no deposition; the equilibrium gap-size distribution is found to decay monotonically, as predicted by their equilibrium analysis. From Eq. (24), this implies that the density of islands around a given island, $c(\ell)$, is uniform even for small values of ℓ. Thus, the positions of the islands are uncorrelated, in contrast with the 2SG protocol (where there are fluctuations for small values of ℓ). On the other hand, the analytical model proposed in Ref. [42] for the island size distribution also decays monotonically and so disagrees with their experimental data. Given that the system remains uniform during growth, the nucleation and aggregation rates are presumably time independent. Consequently, Eq. (29) can be applied to describe the island size distribution. Figure 11 shows the fit found for Eq. (29) with the experimental data reported in Ref. [42]. The agreement given by Eq. (29) is clearly better than that of the equilibrium model of Gambardella et al., especially for small values of s.

ACKNOWLEDGMENTS

Appendix A: kMC Simulations

The kMC simulations were carried in the usual way [71]. Let r_l^i and r_r^i be the hopping rates of the i-th monomer to the left and to the right, respectively. As mentioned in the main text, $r_r^i = D_0 \exp(-\epsilon/(k_B T))$ with $\epsilon = \epsilon_a$, $\epsilon = \epsilon_n$ and $\epsilon = 0$ if the right neighbor is an island, a monomer or an empty site, respectively. The rate r_l^i is defined analogously. At each time step, a list of all monomers is created, and the hopping rates associated with each one are calculated. Then, the sum of the hopping rates $r = \sum_i (r_r^i + r_l^i)$ is calculated, and a uniformly-distributed random number, R, between 0 and r is generated. R determines which particle can move and the associated direction for the corresponding simulation step. For instance, in Fig. 12 $r_r^i < R < r_l^i$; thus, the i-th monomer is selected to move to the next site at its right. Finally, the time is increased by $\log(p)/r$, where p is another uniformly distributed random number between 0 and 1. This procedure is repeated for each time step.
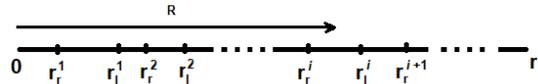

FIG. 12: The uniformly distributed number R determines the particle which might move and the direction of that possible motion.

[1] A. Pimpinelli and T. L. Einstein, Phys. Rev. Lett. **99**, 226102 (2007).
[2] A. Pimpinelli and T. L. Einstein, Phys. Rev. Lett. **104**, 149602 (2010).
[3] M. Li, Y. Han, and J. W. Evans, Phys. Rev. Lett. **104**, 149601 (2010).
[4] T. J. Oliveira and F. D. A. Aarão Reis, Phys. Rev. B **83**, 201405(R) (2011).
[5] J. W. Evans and M. C. Bartelt, Phys. Rev. B **63**, 235408 (2001).
[6] J. G. Amar, M. N. Popescu, and F. Family, Surf. Sci. **491**, 239, (2001).
[7] D. L. González, A. Pimpinelli, and T. L. Einstein, Phys. Rev. E. **84**, 011601 (2011).
[8] J. A. Blackman and P. A. Mulheran, Phys. Rev. **B 54**, 11681 (1996).
[9] K. P. O'Neill, M. Grinfeld, W. Lamb, and P.A. Mulheran, Phys. Rev. E **85**, 021601 (2012).
[10] J. G. Amar and M. N. Popescu, Phys. Rev. B **69**, 033401 (2004).
[11] P. A. Mulheran, K. P. O'Neill, M. Grinfeld, and W. Lamb, Phys. Rev. E **86**, 051606 (2012).
[12] M. Grinfeld, W. Lamb, K. P. O'Neill, and P. A. Mulheran. J. Phys. A: Math. Theor. **45** 015002 (2012).
[13] V. I. Tokar and H. Dreyssé, Phys. Rev. B **80**, 161403(R) (2009).
[14] V. I. Tokar and H. Dreyssé, J. Phys. A: Math. Theor. **50**, 375002 (2017).
[15] F. Shi, Y. Shim, and J. G. Amar, Phys. Rev. E **79**, 011602 (2009).
[16] P. A. Mulheran and D. A. Robbie, Europhys. Lett. **49**, 617 (2000).
[17] J. G. Amar and F. Family, Phys. Rev. Lett. **74**, 2066 (1995).
[18] M. N. Popescu, J. G. Amar, and F. Family, Phys. Rev. B **64**, 205404 (2001).
[19] M. N. Popescu, J. G. Amar, and F. Family, Phys. Rev. B **58**, 1613 (1998).
[20] F. Shi, Y. Shim, and J. G. Amar, Phys. Rev. B **71**, 245411 (2005); **74**, 021606 (2006).
[21] T. J. Oliveira and F. D. A. Aarão Reis, Phys. Rev. B **86**, 115402 (2012).
[22] C. Ratsch, A. Zangwill, P. Šmilauer, and D. D. Vvedensky, Phys. Rev. Lett. **72**, 3194 (1994).
[23] C. Ratsch, Y. Landa, and R. Vardavas, Surf. Sci. **578**, 196 (2005).
[24] J. W. Evans and M. C. Bartelt, Phys. Rev. B **66**, 235410 (2002).
[25] H. Ibach, *Physics of Surfaces and Interfaces* (Springer, Berlin, 2006).
[26] L. Tumbek and A. Winkler, Surface Science **606**, L55 (2012).
[27] T. C. Chang, I. S. Hwang, and T. T. Tsong, Phys. Rev. Lett. **83**, 1191 (1999).
[28] T. C. Chang, K. Chatterjee, S.-H. Chang, Yi-Hsien Lee, and I. S. Hwang, Surface Science **605**, 1249 (2011).
[29] I. S. Hwang, T. C. Chang, and T. T. Tsong, Phys. Rev. Lett. **80** 4229 (1998).
[30] I. S. Hwang, T. C. Chang, and T. T. Tsong, Jpn. J. Appl. Phys. **39**, 4100 (2000).
[31] P. Meakin, in *Phase Transitions and Critical Phenomena*, edited by C. Domb and J. L. Lebowitz (Academic, New York, 1988), Vol. **12**, p. 335.
[32] R. Jullien and M. Kolb, J. Phys. A **17**, L639 (1984).
[33] A. Pimpinelli, L. Tumbek, and A. Winkler, J. Phys. Chem. Lett. **5**, 995 (2014).
[34] E. Loginova, N. C. Bartelt, P. J. Feibelman, and K. F. McCarty, New J. Phys. **10**, 093026 (2008).
[35] E. Loginova, N. C. Bartelt, P. J. Feibelman, and K. F. McCarty, New J. Phys. **11**, 063046 (2009).
[36] J. Ning, D. Wang, D. Han, Y. Shi, W. Cai, J. Zhang, and Y. Hao, J. Cryst. Growth **424**, 55 (2015).
[37] H. S. Mok, A. Ebnonnasir, Y. Murata, S. Nie, K. F. McCarty, C.V. Ciobanu, and S. Kodambaka, Appl. Phys. Lett. **104**, 101606 (2014).

[38] J. Park, J. Lee, J.-H. Choi, D. K. Hwang, and Y.-W. Song, Sci. Rept. **5**, 11839 (2015).

[39] S. M. Binz, M. Hupalo, X. Liu, C. Z. Wang, W.-C. Lu, P. A. Thiel, K. M. Ho, E. H. Conrad, and M. C. Tringides, Phys. Rev. Lett. **109**, 026103 (2012).

[40] J.-S. Lee, S. Sugou, and Y. Masumoto, J. Cryst. Growth **205**, 467 (1999).

[41] J.-S. Lee, M. Sugisaki, H.-W. Ren, S. Sugou, and Y. Masumoto, Physica E **7**, 303 (2000).

[42] P. Gambardella, H. Brune, K. Kern, and V. I. Marchenko, Phys. Rev. B **73**, 245425 (2006).

[43] V. I. Tokar and H. Dreyssé, Phys. Rev. B **76**, 073402 (2007).

[44] F. Picaud, C. Ramseyer, C. Girardet, H. Brune, and K. Kern, Surf. Sci. **553**, (2004).

[45] M. A. Albao, M. M. R. Evans, J. Nogami, D. Zorn, M. S. Gordon, and J. W. Evans, Phys. Rev. B **72**, 035426 (2005).

[46] J. Javorský, M. Setvín, I. Ošt'ádal, P. Sobotík, and M. Kotrla, Phys. Rev. B **79**, 165424 (2009).

[47] M. C. Bartelt and J. W. Evans, Phys. Rev. B **46**, 12675 (1992).

[48] D. L. González, A. Pimpinelli, and T. L. Einstein. Phys. Rev. E **96**, 012804 (2017).

[49] C. Ratsch and J. A. Venables, J. Vac. Sci. Technol. A **21**, S96 (2003).

[50] H. Jónsson, Annu. Rev. Phys. Chem. **51**, 623 (2000).

[51] D. Kandel, Phys.Rev.Lett. **78**, 499 (1997).

[52] R. C. Ball, D. A. Weitz, T. A. Witten, and F. Leyvraz, Phys. Rev. Lett. **58**, 274 (1987).

[53] H. Kallabis, P.L. Krapivsky, and D.E. Wolf, Eur. Phys. J. B **5**, 801-804 (1998).

[54] J. Krug, P. Politi, and T. Michely, Phys. Rev. B **61**, 14037 (2000).

[55] Y. Han, É. Gaudry, T. J. Oliveira, and J. W. Evans, J. Chem. Phys. **145**, 211904 (2016).

[56] Z. Zhang and M. G. Lagally, Science **276**, 377 (1997).

[57] D. L. González, Revista de Ciencias **18**, 81 (2014).

[58] D. L. González, J. Phys. A: Math. Theor. **50**, 035001 (2017).

[59] D. L. González, M. A. Camargo, and J. A. Sánchez, Phys. Rev. E **97**, 052802 (2018).

[60] P. Politi and J. Villain, Phys. Rev. B **54**, 5114 (1996).

[61] C. Castellano and P. Politi, Phys. Rev. Lett. **87**, 056102 (2001).

[62] P. Politi and C. Castellano, Phys. Rev. E **66**, 031605 (2002).

[63] D. L. González, M. A. Camargo, and J. A. Sánchez, Rev. Cienc. **21** (1) (2017).

[64] M. Körner, M. Einax, and P. Maass, Phys. Rev. B **86**, 085403 (2012).

[65] V. I. Tokar and H. Dreyssé, Phys. Rev. E **92**, 062407 (2015).

[66] D. ben-Avraham and S. Havlin, *Diffusion and Reactions in Fractals and Disordered Systems* (Cambridge University Press, 2000).

[67] P. L. Krapivsky, S. Redner and E. Ben-Naim, *A Kinetic View of Statistical Physics*. (Cambridge University Press, 2010).

[68] E. E. Gruber and W. W. Mullins, J. Phys. Chem. Solids **28**, 875 (1967).

[69] D. Walton, J. Chem. Phys. **37**, 2182 (1962).

[70] T. L. Einstein, A. Pimpinelli, and D. L. González, J. Cryst. Growth **401**, 67 (2014).

[71] A. F. Voter, Introduction to the Kinetic Monte Carlo Method, in *Radiation Effects in Solids*, edited by K. E. Sickafus, E. A. Kotomin, and B. P. Uberuaga, NATO Science Series **235** (Springer, Dordrecht, 2007).

[72] Following Ref. [8], the local density of monomers around a given island can be written as $n_1(x) = N_1(1 - \exp(-x/\xi))$, where the capture length ξ is given by Eq. (16). Thus, the monomer density becomes constant for $x \gg \xi$.